

Supporting Information

Gold Nanoparticles with Tailored Size through Ligand Modification for Catalytic Applications

Nidhi Kapil¹, Fabio Cardinale¹, Tobias Weissenberger¹, Panagiotis Trogadas¹, T. Alexander Nijhuis², Michael M. Nigra^{3*} and Marc-Olivier Coppens^{1*}

¹ Centre for Nature Inspired Engineering and Department of Chemical Engineering, University College London, London WC1E 7JE (United Kingdom)

² SABIC Europe, Geleen, Limburg 6167 RD (The Netherlands)

³ Department of Chemical Engineering, University of Utah, Salt Lake City, UT 84112 (USA)

Table of Contents

Experimental	2
Supplementary Figures	4
References	13

Experimental

Materials

Chloro(triphenylphosphine)gold(I) (Sigma Aldrich), chloro(dimethylphenylphosphine)gold(I) (Sigma Aldrich), chloro(trimethylphosphine) gold(I) (Sigma Aldrich), ethanol (Merck), sodium borohydride (Sigma Aldrich), tetraethyl orthosilicate (Sigma Aldrich), tetra-propyl ammonium hydroxide (Merck), tetra-butyl orthotitanate (Merck), lithium tetraborate (Sigma Aldrich), nitric acid (Sigma Aldrich), hydrochloric acid (Sigma Aldrich), poly(tetrafluoroethylene) (Sigma Aldrich), silicon carbide (Alfa Aesar) were received and used as is. Ultra-high-grade propylene was purchased from Air Liquide and ultra-high-purity helium, nitrogen, and oxygen cylinders were purchased from BOC Ltd.

Characterisation

The UV/Vis absorption spectra for gold colloids (dissolved in ethanol) were measured at room temperature with a Cary 4000 UV/Vis spectrophotometer using a quartz cuvette. Diffuse reflectance UV/Vis spectra of the supported powder was studied on the same spectrophotometer equipped with a praying mantis (solid sample cell attachment, Harrick Scientific) using poly(tetrafluoroethylene) as a reference. The transmission electron microscopy (TEM) images were conducted on JEOL 2100 instrument operating at 200 kV. The sample was drop-casted to holey carbon-coated copper grids (EM resolutions) and dried before imaging under the microscope. The particle size distribution was calculated using ImageJ software. For accuracy, 200 particles were measured to determine each of the particle size distributions. The scanning electron microscopy (SEM) was performed using a Hitachi-S3400N electron microscope. X-ray diffraction was performed on a Stoe STADI-P diffractometer with Cu K α radiation ($\lambda = 0.15406$ nm) working at 40 kV and 30 mA. Nitrogen adsorption and desorption isotherms of TS-1 samples were measured using a Quantachrome Autosorb iQ2 automated gas sorption analyser. Prior to the measurement, samples were outgassed at 380 °C for 8 hours. Thermogravimetric analysis (TGA) of catalyst powder were carried out in a Perkin Elmer thermal analyser under flowing air. The temperature was increased at a rate of 10 °C/min from room temperature to 800 °C. The final gold loading was determined using a Varian 720 ICP-OES. Samples were prepared by the flux melting technique, using lithium tetraborate, followed by dissolution in nitric acid and aqua regia.^{1, 2}

Synthesis of gold nanoparticles – P1

The P1 nanoparticles were synthesised using a one-step methodology. Briefly, 25.1 mg of chloro(triphenylphosphine) gold(I) was dissolved in 50 mL of ethanol in a 100 mL round bottom flask. After stirring for 15 min, 4 eq. of finely ground NaBH₄ w.r.t. Au was added to the reaction mixture. This mixture was stirred for 2h at room temperature. The colour of the solution changed from colourless to brown at the end.

Synthesis of gold nanoparticles – P2

The P2 nanoparticles were synthesised using a one-step methodology. Briefly, 18.8 mg of chloro(dimethylphenylphosphine) gold(I) was dissolved in 50 mL of ethanol in a 100mL round bottom flask. After stirring for 15 min, 4 eq. of finely ground NaBH₄ w.r.t. Au was added to the reaction mixture. This mixture was stirred for 2 h at room temperature. The colour of the solution changed from colourless to pink at the end.

Synthesis of gold nanoparticles – P3

The P3 nanoparticles were synthesised using a one-step methodology. Briefly, 15.6 mg of chloro(trimethylphosphine) gold(I) was dissolved in 50 mL of ethanol in a 100mL round bottom flask. After stirring for 15 min, 4 eq. of finely ground NaBH₄ w.r.t. Au was added to the reaction mixture. This mixture was stirred for 2 h at room temperature. The colour of the solution changed from colourless to purple at the end.

Synthesis and characterisation of TS-1

TS-1, used as a support, was synthesised according to a method reported previously in the literature.³ The physical properties of the TS-1 sample are determined using XRD, N₂ physisorption, HRTEM, SEM, and DR-UV/Vis spectroscopy. The powder XRD pattern (Fig. S1, ESI) of this sample shows typical MFI reflections and an absence of phase impurities. The DR-UV/Vis spectra shown in Fig. S2 (ESI) reveal a characteristic peak at 205 nm assigned to isolated tetrahedrally coordinated titanium (Ti⁴⁺) species present within the zeolite framework.^{4,5} The nitrogen adsorption and desorption isotherms (Fig. S3, ESI) exhibit a typical type I isotherm according to the IUPAC classification, which is a characteristic for microporous materials with typical micropore volume and BET surface area as expected for TS-1 zeolites.⁶ Fig. S4, S5 (ESI) show a representative SEM and HRTEM image of TS-1, indicating a highly crystalline and uniform material, which agrees well with the XRD pattern.

Synthesis of supported gold catalysts

The as-synthesised AuNPs were directly immobilised onto the TS-1 support. 1 g of the TS-1 powder was placed in a round bottom flask. 50 mL ethanolic solution of AuNPs (P1, P2, P3) was poured onto the supports to obtain 0.5 wt. % final Au loading. Ethanol was removed using a rotary evaporator at 45 °C under vacuum. After the removal of the solvent, brown, pink and purple coloured powder was obtained for Au-P1/TS-1, Au-P2/TS-1 and Au-P3/TS-1 catalysts, respectively. After drying, the solid powder was dispersed in hexane and washed 3 times through the frit using a water and hexane (1:1, by volume) mixture. The ligand removal was performed using a non-thermal O₂ plasma at room temperature. The catalyst powder was placed in a plasma chamber (Henniker HPT-200) operated at 750 VA and 0.5 mbar pressure for 30 min.

Catalytic tests

The catalysts were tested for direct gas phase propylene epoxidation in a fixed packed bed reactor. 0.5 g of catalyst powder diluted with 2.5 g of silicon carbide (SiC/catalyst wt. ratio = 5) was loaded into the vertical quartz reaction tube (outer diameter 9 mm, wall thickness 1.5 mm) and placed inside the tubular furnace (Carbolite Gero), equipped with a fixed K-type probe thermocouple to measure the reaction temperature. Afterwards, a gas stream composed of 10% C₃H₆, 10% H₂, 10% O₂ in 70% He was introduced as a reaction feed into the reactor at a total flow rate of 66.67 mL min⁻¹, resulting in a gas hourly space velocity (GHSV) of 8000 mL g_{cat}⁻¹h⁻¹. The catalysts were tested at a reaction temperature of 225 °C. The concentrations of reactants and products were analysed by online gas chromatography (GC, Shimadzu). The oxygenates, such as propylene oxide, ethanal, propanal, acetone and acrolein, along with CO₂, H₂O and propylene were separated using Porapak T packed column and analysed via a flame ionisation detector (FID). The hydrogen, oxygen and CO were separated using a Molsieve 5Å column and analysed via a thermal conductivity detector (TCD) detector. A blank test was performed, which confirmed that no

PO was formed in the absence of catalyst. The C_3H_6 conversion, PO formation rate, PO selectivity and H_2 efficiency were determined and calculated as follows:⁷

$$C_3H_6 \text{ conversion (\%)} = \frac{\frac{1}{3}F_{CO_x}^{out} + \frac{2}{3}F_{ethanal}^{out} + \sum F_{C_3\text{oxygenates}}^{out}}{F_{C_3H_6}^{in}} \times 100$$

$$\text{PO production rate (g}_{PO}\text{h}^{-1}\text{kg}_{\text{cat}}^{-1}\text{)} = \frac{F_{PO}^{out}}{\text{catalyst weight}} \times M_{PO} \times 60$$

$$\text{PO selectivity (\%)} = \frac{F_{PO}^{out}}{\frac{1}{3}F_{CO_x}^{out} + \frac{2}{3}F_{ethanal}^{out} + \sum F_{C_3\text{oxygenates}}^{out}} \times 100$$

$$H_2 \text{ efficiency (\%)} = \frac{F_{H_2}^{out}}{F_{H_2}^{in} - F_{H_2}^{out}} \times 100$$

Here, F_i is the molar flow rate of the generic i_{th} species, in mol min^{-1} , catalyst weight is in kg, and M_{PO} is the molar mass of propylene oxide in g/mol.

Supplementary Figures

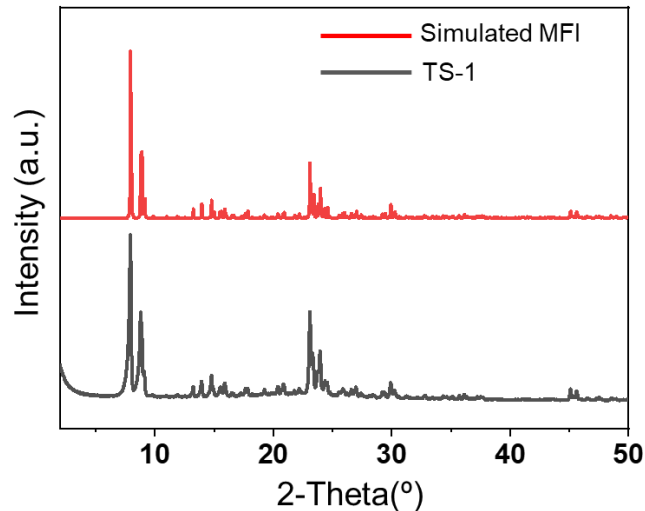


Fig. S1. Powder X-ray diffraction pattern of simulated MFI and TS-1 support.

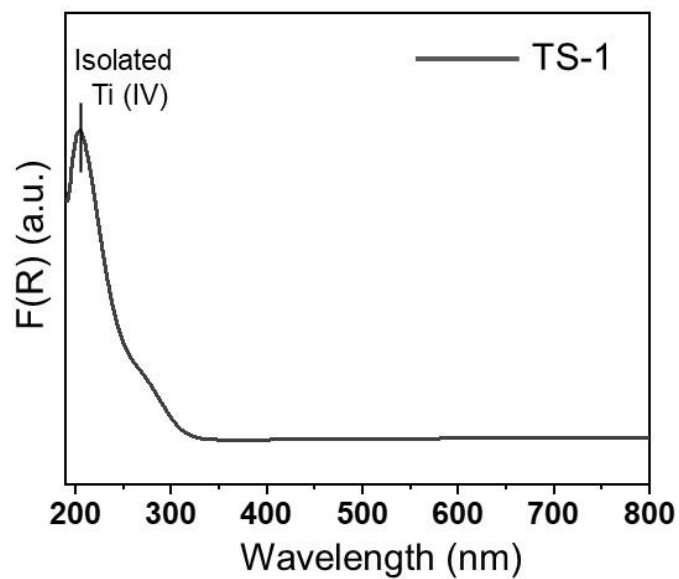
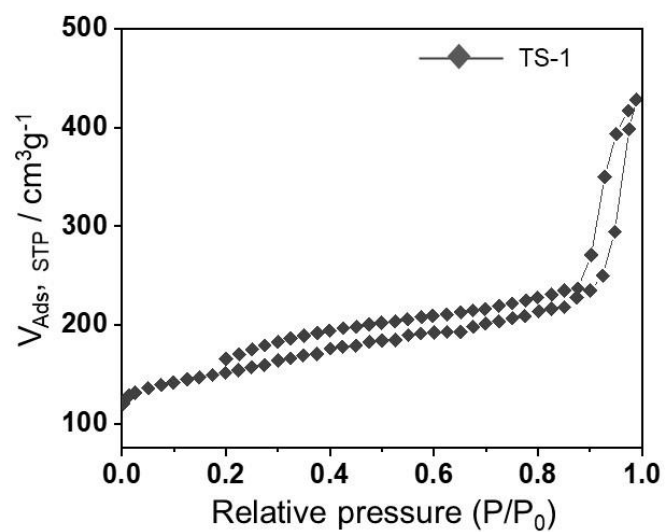


Fig. S2. DR-UV/Vis spectrum of TS-1 support.



Sample	Surface Area (m ² /g)	Micropore Vol. (cm ³ /g)
TS-1	563	0.14

Fig. S3. N₂ physisorption isotherms of TS-1 support.

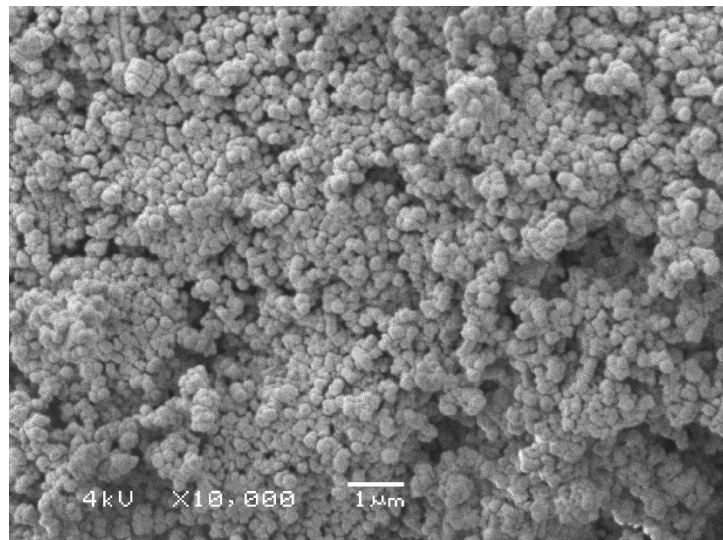


Fig. S4. SEM image of TS-1.

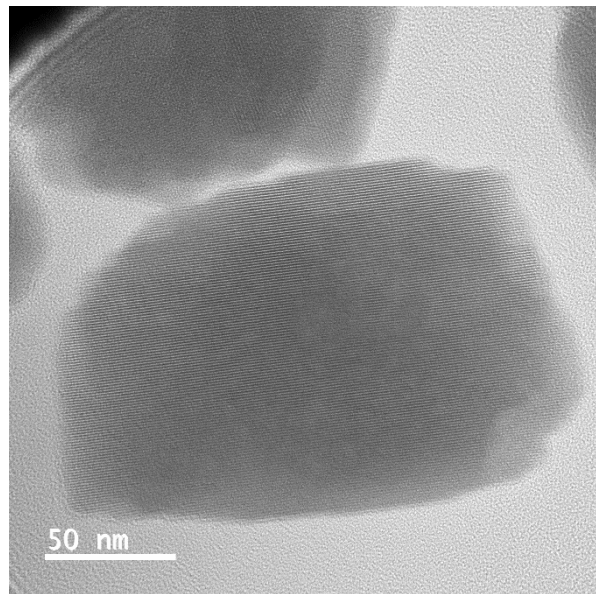


Fig. S5. HRTEM image of TS-1.

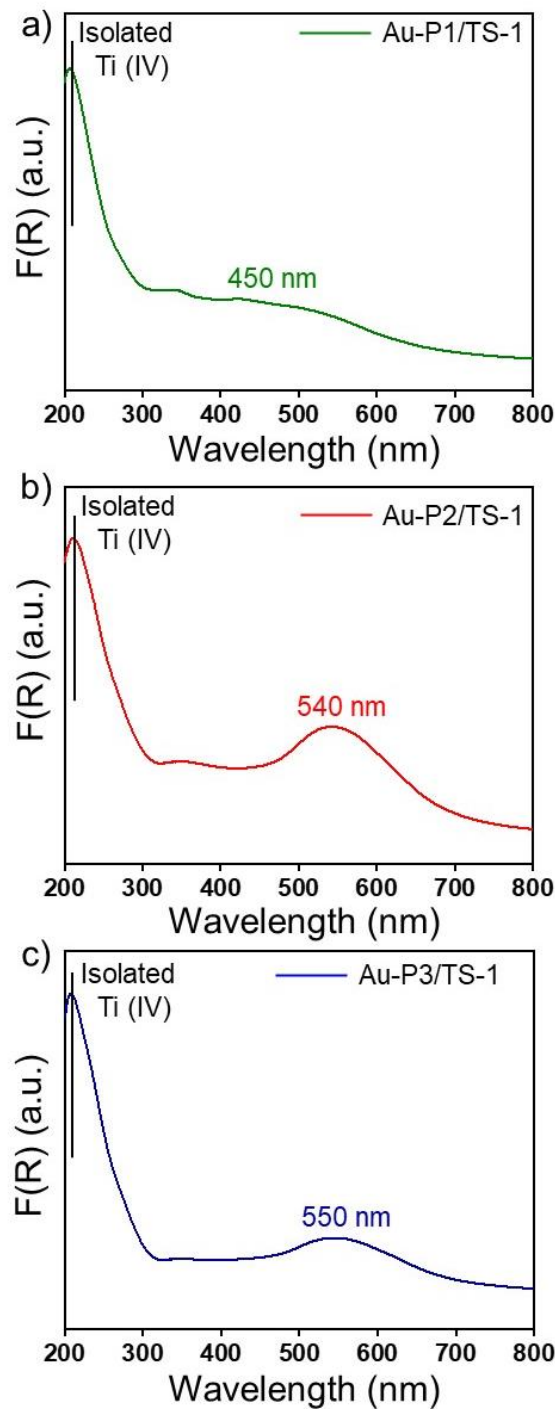


Fig. S6. DR-UV/Vis spectra of Au immobilised onto TS-1, using Au nanoparticles synthesised using precursor a) P1, b) P2 and c) P3.

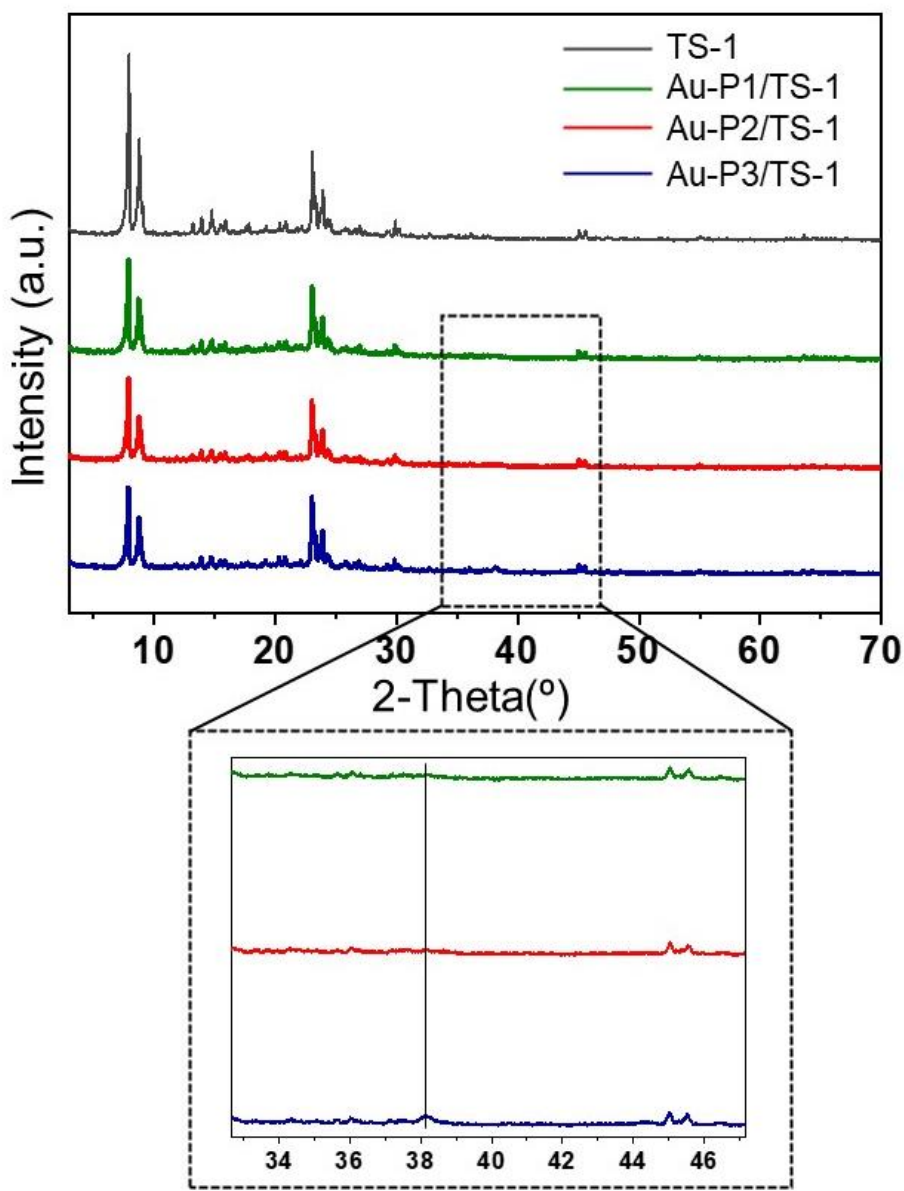


Fig. S7. Powder X-ray diffraction patterns of TS-1, Au-P1/TS-1, Au-P2/TS-1 and Au-P3/TS-1. The bottom image is a magnification of to the 2θ range from 32.6 to 47° . The Au-P3/TS-1 sample with the largest Au particle size of ca. 10 nm shows a small peak at 38.1° , corresponding to fcc Au(1 1 1).⁸

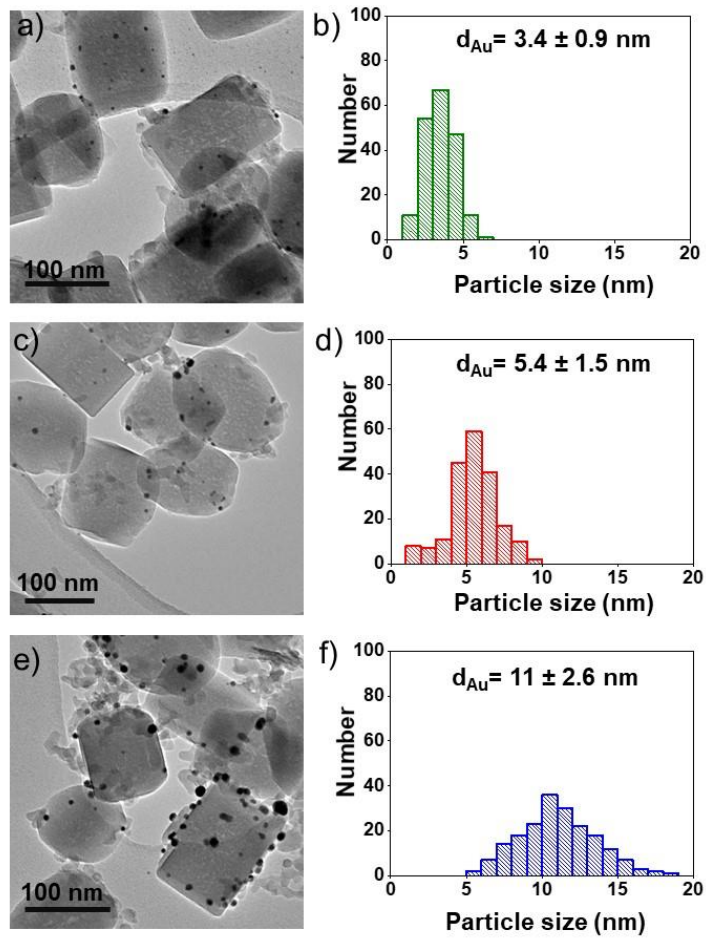


Fig. S8. TEM and corresponding particle size distribution for plasma treated catalyst: a, b) Au-P1/TS-1, c, d) Au-P2/TS-1 and e, f) Au-P3/TS-1.

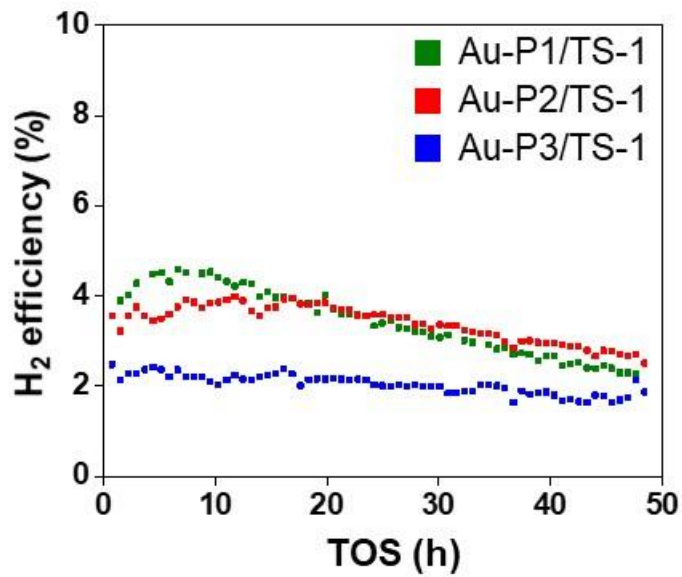


Fig. S9. H₂ efficiency of plasma treated Au-P1/TS-1, Au-P2/TS-1 and Au-P3/TS-1 catalysts.

Table. S1. Catalytic performance for propylene epoxidation over Au/TS-1 catalysts where Au/TS-1 catalyst is prepared using different synthesis methods, listed as DP (deposition precipitation), IL (ionic liquid-enhanced immobilisation), SEI (sol-enhanced immobilisation), and DI (direct immobilisation).

Catalyst Au loading%- Au/TS-1 (Si Ti ratio)	Preparat ion method	Average Au particle size (nm)	C ₃ H ₆ conversion (%)	Selectivity to PO (%)	PO Production Rate (g _{POh⁻¹} kg _{cat⁻¹})	Reaction Temperature (°C)	Reaction conditions	Reference
1% Au/TS-1 (-)	DP	3-10	0.3	>99	3.2	70	a	3
1% Au/TS-1 (-)	DP	3-10	2.0	50	21.4	200	a	3
0.5% Au/TS- 1(35)	DP	3.5	0.8	70.9	9.2	300	b	9
0.5% Au/TS- 1(35)	IL	3.6	10.1	72.1	120	300	b	9
0.5% Au/TS- 1(35)	IL	3.6	2.7	81	40	220	b	9
0.10% Au/TS-1 (99)	DP	2.9	5	88	160	200	c*	10
0.25% Au/TS-1 (-)	SEI	3.6	1.12	77.2	20.17	200	d	11
2.50% Au/TS- 1(-)	DP	5.6	0.55	82.8	10.59	200	d	11
0.5% Au-P1/TS- 1 (60)	DI	3.4	1.1	78	15	225	e	This work
0.5% Au-P1/TS- 1 (60)	DI	5.4	0.9	78	12	225	e	This work
0.5% Au-P1/TS- 1 (60)	DI	11	0.2	60	3.5	225	e	This work

a) Feed gas C₃H₆:H₂:O₂:N₂ = 10:10:10:70 (vol%); space velocity 8000 mL g_{cat⁻¹} h⁻¹

b) Feed gas C₃H₆:H₂:O₂:N₂ = 1/1/1/7 (vol%); space velocity 7000 mL h⁻¹ kg_{cat⁻¹}

c) Feed gas C₃H₆:H₂:O₂:N₂ = 3.5/3.5/3.5/24.5 mL min⁻¹, space velocity 14,000 mL h⁻¹kg_{cat⁻¹}
*The catalyst decayed within 10 hours of the reaction.

d) Feed gas C₃H₆:H₂:O₂:Ar= 1.5/1.5/1.5/10.5 mL min⁻¹, space velocity 9000 mL g_{cat⁻¹} h⁻¹

e) Feed gas C₃H₆:H₂:O₂:He= 10:10:10:70 (vol%), space velocity 8000 mL g_{cat⁻¹} h⁻¹

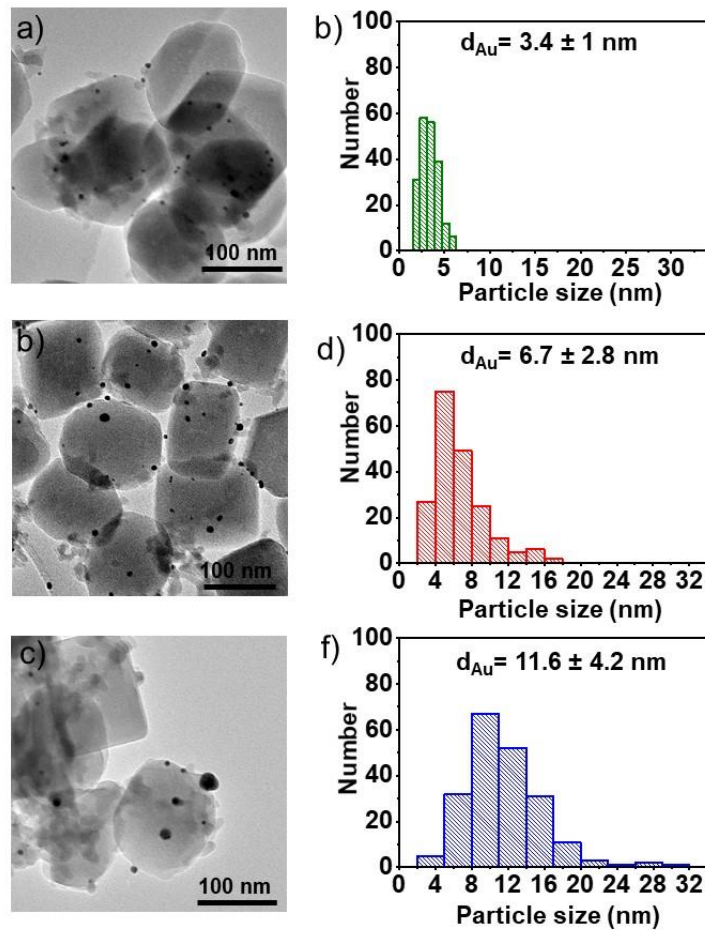


Fig. S10. TEM and corresponding particle size distribution of spent catalyst: a, b) Au-P1/TS-1, c, d) Au-P2/TS-1 and e, f) Au-P3/TS-1.

References

1. C. Ingamells, *Anal. Chim. Acta*, 1970, **52**, 323-334.
2. A. Wittmann and F. Kop, *Spectrochimica Acta Part B: Atomic Spectroscopy*, 1986, **41**, 73-79.
3. T. A. Nijhuis, B. J. Huizinga, M. Makkee and J. A. Moulijn, *Industrial & engineering chemistry research*, 1999, **38**, 884-891.
4. P. Wu, T. Tatsumi, T. Komatsu and T. Yashima, *The Journal of Physical Chemistry B*, 2001, **105**, 2897-2905.
5. P. Ratnasamy, D. Srinivas and H. Knözinger, in *Advances in Catalysis*, Academic Press, 2004, vol. 48, pp. 1-169.
6. M. Thommes, K. Kaneko, A. V. Neimark, J. P. Olivier, F. Rodriguez-Reinoso, J. Rouquerol and K. S. Sing, *Pure Appl. Chem.*, 2015, **87**, 1051-1069.
7. T. Hayashi, K. Tanaka and M. Haruta, *J. Catal.*, 1998, **178**, 566-575.
8. T. Ayvali, L. Ye, S. Wu, B. T. Lo, C. Huang, B. Yu, G. Cibin, A. I. Kirkland, C. Tang and A. A. Bagabas, *J. Catal.*, 2018, **367**, 229-233.
9. M. Du, G. Zhan, X. Yang, H. Wang, W. Lin, Y. Zhou, J. Zhu, L. Lin, J. Huang and D. Sun, *J. Catal.*, 2011, **283**, 192-201.

10. W.-S. Lee, M. Cem Akata, E. A. Stach, F. H. Ribeiro and W. Nicholas Delgass, *J. Catal.*, 2012, **287**, 178-189.
11. N. Li, Y. Chen, Q. Shen, B. Yang, M. Liu, L. Wei, W. Tian and J. Zhou, *J. Solid State Chem.*, 2018, **261**, 92-102.